

**How to Cite:**

Banupriya, K., & Girija, R. (2022). Design, efficient synthesis, docking studies and quantum calculations of Schiff bases. *International Journal of Health Sciences*, 6(S4), 11668–11680. <https://doi.org/10.53730/ijhs.v6nS4.11261>

# Design, efficient synthesis, docking studies and quantum calculations of Schiff bases

**K. Banupriya**

Research Scholar, Department of Chemistry, Queen Mary's College, Chennai

**Dr. R. Girija**

Assistant Professor, Department of Chemistry, Queen Mary's College, Chennai

**Abstract**---Schiff bases (2a-i) have been synthesized. Their chemical structures were characterized by IR, <sup>1</sup>H NMR, <sup>13</sup>C NMR and mass spectral analysis. The synthesized compounds were subjected to docking studies using Schrodinger Meastro 12.4. The results pointed out that compounds 2f, 2h and 2c were explored superior inhibition activity with the protein 4OD9. Further, the results of QM studies of these synthesized compounds indicated the importance of weakly polar component of surface area, hydrophobicity and ionization potential parameters in defining their anticancer activity.

**Keywords**---Schiff bases, maestro 12.4, docking, anticancer activity.

## Introduction

Schiff bases are condensation products of primary amines with carbonyl compounds. A common structural feature of these compounds is azomethine group with the general formula  $RHC=N-R_1$ , where R and R<sub>1</sub> are alkyl, aryl, cycloalkyl or heterocyclic groups, which may be variously substituted [1]. Several studies [2-4] showed that the presence of a lone pair of electrons in a sp<sup>2</sup> Hybridized orbital of the nitrogen atom of the azomethine group is of considerable chemical and biological importance. Schiffbase compounds containing an imino group ( $-C=N-$ ) are potential anticancer drugs. Due to the straight forward preparation, synthetic flexibility and the special property of the C=N group, Schiff bases are generally excellent chelating agents [5,6], especially when a functional group like -OH is present close to the azomethine group. Schiff bases have also been reported to show biological properties, such as antibacterial and antifungal activities [7-9].

Cancer is the most common cause of mortality in most parts of the world[10] and currently is the most common impediment to achieving desirable life expectancy in most countries Breast cancer is one of the lethal diseases worldwide. According

to the Malaysia National Cancer Registry Report (MNCR 2007-2011), 17.7% from 103,507 new cases of cancer detected throughout Malaysia was breast cancer. The current treatments available are chemotherapy and hormone therapy using tamoxifen. However, it causes some side effects, which includes extreme fatigue, loss appetite, and depression. Therefore, there is a need for more targeted and less side-effect anti-cancer drug. Substituted Schiff bases are well known for their profound anticancer activity[11].

This article reports the efficient synthesis of the mentioned nitrogen containing heterocycles using ethanol as a solvent by a conventional synthetic route. Along with routine spectroscopic studies to ascertain the structure, an attempt to obtain single-crystals of as many compounds as possible in order to understand structural features, bond length, bond angles and atomic spacing are presented. Molecular docking studies were carried out to identify the potential binding affinities and the mode of interaction of the compounds against protein 4OD9.

## Chemistry

The general schematic representation describing the routes of syntheses is furnished in Scheme 1. (1E,4E)-1,5-diphenylpenta-1,4-dien-3-one were prepared by the condensation reaction of benzaldehyde with respective ketones in the presence of sodium hydroxide in Water/ ethanol medium stirred for 4hrs. N-((1E,4E)-1,5-bis(2,6-dichloro-4-methylphenyl)penta-1,4-dien-3-ylidene)-1-(2-chlorophenyl)methanamine are synthesized by refluxing (1E,4E)-1,5-diphenylpenta-1,4-dien-3-one with respective (2-chlorophenyl)methanamine in the presence of sodium hydroxide in ethanol medium for 24 h. All the synthesized compounds were characterized by analytical and spectral (Mass, IR,  $^1\text{H}$  and NMR) data. The physical and analytical data of the Schiff bases (2a-i) are presented in Table 1. The stereochemistry of all the synthesized Schiff bases are established using  $^1\text{H}$  NMR spectral data.

### Schematic diagram 1

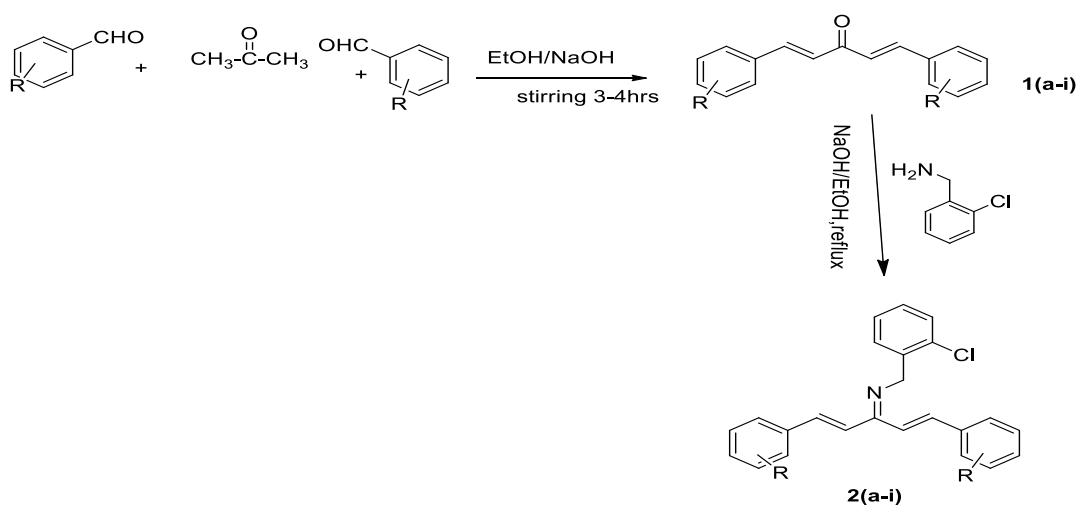


Table 1  
Physical data of Schiff bases (2a-i)

| Compound | R                     | Reaction Time(hrs) | Yield( %) | m.p <sup>o</sup> C | Mass( m/z) | Elemental Analysis |      |       |       |       |
|----------|-----------------------|--------------------|-----------|--------------------|------------|--------------------|------|-------|-------|-------|
|          |                       |                    |           |                    |            | C                  | H    | N     | O     | S     |
| 2a       | H                     | 24                 | 87        | 77-79              | 357.13     | 80.55              | 5.63 | 3.91  | -     | -     |
| 2b       | 2,6-dichloro-4-methyl | 24                 | 87        | 71-73              | 521.00     | 59.63              | 3.85 | 2.67  | -     | -     |
| 2c       | 4-methoxy             | 24                 | 88        | 76-78              | 417.15     | 74.72              | 5.79 | 3.35  | 7.66  | -     |
| 2d       | 3,4,5-trimethoxy      | 24                 | 85        | 73-75              | 537.19     | 66.97              | 5.99 | 2.60  | 17.84 | -     |
| 2e       | 4-methyl              | 24                 | 86        | 79-80              | 385.16     | 80.92              | 6.27 | 3.63  | -     | -     |
| 2f       | 2,4-dimethyl          | 24                 | 86        | 78-80              | 413.19     | 81.24              | 6.82 | 3.38  | -     | -     |
| 2g       | 2-nitro-4-bromo       | 24                 | 86        | 77-79              | 602.92     | 47.59              | 2.66 | 6.94  | 10.57 | -     |
| 2h       | pyridine aldehyde     | 24                 | 86        | 76-78              | 359.12     | 73.43              | 5.04 | 11.68 | -     | -     |
| 2i       | thiophenaldehyde      | 24                 | 87        | 77-79              | 369.04     | 64.93              | 4.36 | 3.79  | -     | 17.34 |

## Experimental Section

### 1-(2-chlorophenyl)-N-((1E,4E)-1,5-diphenylpenta-1,4-dien-3-ylidene)methanamine(2a)

Yield-87%,m.p-77-79<sup>o</sup> C, <sup>1</sup>H NMR-  $\delta$  2.2-2.5 (s,methylene proton), 4.5-5.7 (d,ethylene proton),6.05-6.75(d,ethylene proton) ,6.85-7.90(m,aromatic proton), <sup>13</sup>C NMR-  $\delta$  55.30(methylcarbon),127.66,127.89,128.13,128.56,128.78,129.48,129.90,130.57,130.77, 132.71,134.54 (aromatic carbons), 159.40(CN carbon), IR(KBR)- 1654,1604,870 cm<sup>-1</sup>, Mass (m/z)-357.13.

### N-((1E,4E)-1,5-bis(2,6-dichloro-4-methylphenyl)penta-1,4-dien-3-ylidene)-1-(2-chlorophenyl)methanamine(2b)

Yield-87%,m.p-71-73<sup>o</sup> C, <sup>1</sup>H NMR-  $\delta$  2.1-2.6 (s,methylene proton),3.6-3.9 (s, methoxy proton), 4.6-5.8 (d,ethylene proton),6.01-6.70(d,ethylene proton) ,6.80-8.10(m,aromatic proton) , <sup>13</sup>C NMR-  $\delta$  55.38(methyl carbon),61.71(methoxy carbon),127.63,127.88,128.04,128.67,128.83,129.38,129.70,130.38,130.77,132.91,134.63 (aromatic carbons), 159.42(CN carbon), IR(KBR)- 1654,1200,1604 cm<sup>-1</sup>, Mass (m/e)-521.00.

### N-((1E,4E)-1,5-bis(4-methoxyphenyl)penta-1,4-dien-3-ylidene)-1-(2-chlorophenyl)methanamine(2c)

Yield-88%,m.p-76-78<sup>o</sup> C, <sup>1</sup>H NMR-  $\delta$  2.1-2.6 (s,methylene proton),3.6-3.9 (s, methoxy proton), 4.6-5.8 (d,ethylene proton),6.01-6.70(d,ethylene proton) ,6.80-8.10(m,aromatic proton) , <sup>13</sup>C NMR- $\delta$ 55.38(methyl carbon),61.71(methoxy carbon),127.63,127.88,128.04,128.67,128.83,129.38,129.70,130.38,130.77,132.91,134.63 (aromatic carbons), 159.42(CN carbon), IR(KBR)- 1654,1200,1604,872 cm<sup>-1</sup>, Mass (m/z)-417.15.

**1-(2-chlorophenyl)-N-((1E,4E)-1,5-di-*p*-tolylpenta-1,4-dien-3-ylidene)methanamine(2d)**

Yield-87%, m.p-73-75<sup>o</sup> C, <sup>1</sup>H NMR- δ 2.5-2.8 (s, methylene proton), 3.1-3.3 (s, methyl proton), 4.7-5.8 (d, ethylene proton), 6.13-6.89 (d, ethylene proton), 6.98-8.09 (m, aromatic proton), <sup>13</sup>C NMR- 55.30 (methyl carbon), 127.60, 127.78, 128.24, 128.57, 128.83, 129.57, 129.78, 130.40, 130.78, 132.4, 134.73 (aromatic carbons), 159.32 (CN carbon), IR (KBR)- 1654, 1200, 1604, 870 cm<sup>-1</sup>, Mass (m/z)-537.19.

**N-((1E,4E)-1,5-bis(2,4-dimethylphenyl)penta-1,4-dien-3-ylidene)-1-(2-chlorophenyl)methanamine(2e)**

Yield-89%, m.p-78-80<sup>o</sup> C, <sup>1</sup>H NMR- δ 2.7-2.9 (s, methylene proton), 3.2-3.6 (s, methyl proton), 4.5-5.9 (d, ethylene proton), 6.25-6.78 (d, ethylene proton), 7.01-8.09 (m, aromatic proton), <sup>13</sup>C NMR- δ 55.40 (methyl carbon), 127.59, 127.57, 128.33, 128.59, 128.88, 129.37, 129.57, 130.45, 130.67, 132.39, 134.65 (aromatic carbons), 159.42 (CN carbon), IR (KBR)- 1210, 1624, 860 cm<sup>-1</sup>, Mass (m/z)-385.16

**N-((1E,4E)-1,5-bis(4-bromo-2-nitrophenyl)penta-1,4-dien-3-ylidene)-1-(2-chlorophenyl)methanamine(2f)**

Yield-88%, m.p-78-80<sup>o</sup> C, <sup>1</sup>H NMR- δ 2.5-2.8 (s, methylene proton), 4.1-5.3 (d, ethylene proton), 6.05-6.68 (d, ethylene proton), 6.89-8.23 (m, aromatic proton), <sup>13</sup>C NMR- δ 55.5 (methyl carbon), 127.58, 127.36, 128.57, 128.65, 128.80, 129.54, 129.87, 130.27, 130.45, 132.83, 134.72 (aromatic carbons), 159.39 (CN carbon), IR (KBR)- 1211, 1624, 1450, 913 cm<sup>-1</sup>, Mass (m/z)-413.19.

**N-((1E,4E)-1,5-bis(3,4,5-trimethoxyphenyl)penta-1,4-dien-3-ylidene)-1-(2-chlorophenyl)methanamine(2g)**

Yield-89%, m.p-77-79<sup>o</sup> C, <sup>1</sup>H NMR- δ 2.1-2.7 (s, methylene proton), 3.6-3.9 (s, methoxy proton), 4.6-5.8 (d, ethylene proton), 6.05-6.65 (d, ethylene proton), 6.91-8.109 (m, aromatic proton), <sup>13</sup>C NMR- δ 55.40 (methyl carbon), 61.69 (methoxy carbon), 127.53, 127.92, 128.24, 128.51, 128.96, 129.03, 129.85, 130.45, 130.87, 133.30, 134.83 (aromatic carbons), 159.52 (CN carbon), IR (KBR)- 2830, 1654, 1200, 1604, 872 cm<sup>-1</sup>, Mass (m/z)- 602.92

**1-(2-chlorophenyl)-N-((1E,4E)-1,5-di(pyridine-3-yl)penta-1,4-dien-3-ylidene)methanamine(2h)**

Yield-88%, m.p-76-78<sup>o</sup> C, <sup>1</sup>H NMR- δ 2.21-2.53 (s, methylene proton), 4.7-5.69 (d, ethylene proton), 6.15-6.64 (d, ethylene proton), 6.85-7.90 (m, aromatic proton), <sup>13</sup>C NMR- δ 55.35 (methyl carbon), 127.43, 127.53, 128.10, 128.44, 128.80, 129.48, 129.90, 130.5

7,130.77,132.60,134.594 (aromatic carbons), 159.39(CN carbon), IR(KBR)-1644,1624,869  $\text{cm}^{-1}$ , Mass (m/z)-359.12.

**1-(2-chlorophenyl)-N-((1E,4E)-1,5-di(thiophen-3-yl)penta-1,4-dien-3-ylidene)methanamine(2i)**

Yield-87%, m.p-77-79 $^{\circ}$  C,  $^1\text{H}$  NMR-  $\delta$  2.2-2.5 (s, methylene proton), 4.5-5.7 (d, ethylene proton), 6.05-6.75 (d, ethylene proton), 6.85-7.90 (m, aromatic proton),  $^{13}\text{C}$  NMR- 85.5.30 (methyl carbon), 127.66, 127.89, 128.13, 128.56, 128.78, 129.48, 129.90, 130.57, 130.77, 132.71, 134.54 (aromatic carbons), 159.40 (CN carbon), IR(KBR)-1654, 1604, 870  $\text{cm}^{-1}$ , Mass (m/e)-369.04.

## **Molecular docking studies**

### **Computational section Docking Studies**

The docking studies of the above 9 compounds with the protein have been carried out by the application LIGAND DOCKING in the module GLIDE of SCHRODINGER software. By the help of this tool we can predict the best binding interaction between the ligand and the protein. Creating an output directory for every work is a must while working in Schrodinger. Before initiating the ligand preparation, the structures have to be converted into maestro format (.mae format) from .mol format. The structures of the 9 compounds have been drawn with the help of the, CHEMDRAW ULTRA 12.0 tool. Each structure has been imported into the MAESTRO 21. from the project table and are then exported from the mol format to the .mae format.

### **Ligand and protein preparation**

#### **Ligand Preparation**

Ligand Preparation LigPrep or ligand preparation is an application where we generate a simple 2D structure to 3D structure which includes the generation of the tautomeric, stereochemical and ionization variations. LigPrep helps in generating an accurate 3D molecular model. The important characteristic of LigPrep application is the energy minimization with optimized potentials for liquid simulations-2005 (OPLS\_2005) as the applied force field which filters customized ligands which can thus be used for further computational analysis. All the 18 ligands have been minimized using Schrödinger suite, whose corresponding results are given in the table 1. The output folder for LigPrep will be displayed as out.maegz [12].

#### **Impact Minimization**

The output folder of LigPrep is used as the input folder for impact minimization. The impact minimization is performed with the help of IMPACT module in which we have a tool called minimization. Among many conformers obtained in the LigPrep, the conformer with least potential energy will be minimized with the help

of impact minimization under the applied OPLS\_2005 force field. The significance of impact minimization is to observe the Lennard Jones Energy, which should be in negative [13].

### **Protein Preparation**

The protein was retrieved from PDB (<http://www.pdb.org>) with the PDB id 4OD9. The ProPrep was processed with the help of the protein preparation wizard from the workflows option of the Schrodinger suite. The force field applied for the preparation of the protein is optimized potentials for liquid simulations-2005 (OPLS\_2005). The water molecules, hetero atoms, residues were deleted while one of the chains is retained along with H-bond. The active site of the protein is identified by the help of PDBCASTp and Q-site finder [14].

### **Grid Generation**

The receptor-grid is generated by the help of the module glide. Grid generation represents the physical properties like volume of the receptor (specifically the active site) that is needed for carrying out the ligand-docking process. Import the output file of the protein preparation; also define the receptor, active site, the positional constraints, and then monitor the generation of the grid calculation. The generated receptor grid is used for the comparative docking studies conducted in ligand docking procedure[15].

### **Docking**

The docking has been carried out by the application LIGAND DOCKING which is present in the module GLIDE12.1 version in the extra precision (XP) mode for clear and accurate details along with Epik state penalties to docking score. Select the selected entries for the ligand to be docked. Also load the output file of the grid generated. The output files of impact minimization of all the compounds are taken as the input files for the docking process. The docking of each compound along with the grid will be carried out which generates conformational changes with respect to the active site of the protein(PDB ID- 4OD9). The glide scores or docking scores will be displayed in a text document. Thus, the ligand which has the least glide score will be considered to have the best docked pose or best glide score.

### **Result and Discussion**

Molecular docking is a tool used in computer aided structure based rational drug design. It is designed to predict how a small molecule binds to a target protein with known 3D structure, and binding energies determined. Also the position of the ligand in the hosts binding site can be visualized. It is helpful for developing better drug with improved activity. The docking score is measure of strength of the non-covalent interaction or binding affinity between two molecules after they have been docked[16-18]. In calculating the docking score, the small organic molecule or ligand is considered as a rigid structure and its interactions with protein receptors are recorded and expressed in terms of energy associated with such interactions. In calculations of the Glide energy value, the conformational,

orientational, and positional space of the docked ligand are taken into consideration [19-20]. Thus, the Glide energy value is obtained with torsionally flexible energy optimization where the ligand is a flexible entity and all its possible geometrical orientations are considered. Hence, the Glide energy value is a more reliable, enhanced, and realistic approach to investigate the docking process. Both docking score or docking and Glide energy are free energy values and expressed in kcal mol<sup>-1</sup>. All the synthesized compounds exhibited good Glide energy and docking scores towards the receptor active pocket, and bind to the active site of the amino acid residue with H-bonding very close to the standard drug Capecitabine (Table 7). Compound 2e showed the highest docking score and a Glide energy lower than that of standard doxorubicin. Its hydrogen bonding distances to amino acids VAL31 and HIS56 are comparatively shorter compared to those found in Capecitabine. Compound 2e can be considered to be the best docked ligand with the highest docking score and lowest Glide energy. The compounds 2h, 2a showed docking scores very close to the standard drug, but Glide energies were found to be comparatively lower. Compounds 2b, 2c, 2d, 2f, 2g, 2i have moderate docking scores and Glide energies. In this study compound 2e showed the shortest hydrogen bonding distance of 1.85 Å, 2.44 Å with the amino acid likely due to presence of the more electronegative atom. Docking score results shown in table 2 and interaction of the compounds shown fig(1-4).

Table2. Docking Results of the compounds

| COMPOUND S   | DOCKING SCORE | GLIDE ENERGY | NO.OF RESIDUES | AMINO ACIDS                | BOND LENGTH      |
|--------------|---------------|--------------|----------------|----------------------------|------------------|
| 2a           | -5.964        | -40.683      | 1              | TYR78                      | -                |
| 2b           | -5.485        | -43.267      | 2              | TRP40, TYR16               | -                |
| 2c           | -4.024        | -41.021      | 1              | TRP40                      | -                |
| 2d           | -5.401        | -38.73       | -              | -                          | -                |
| 2e           | -7.648        | -34.663      | 2              | VAL31, HIS2.44             | 1.85, 2.44       |
| 2f           | -4.907        | -48.012      | 4              | TRP40, SER80, GLY79, TYR78 | 2.84, 3.25, 3.33 |
| 2g           | -5.273        | -37.62       | 1              | VAL31                      | 2.29             |
| 2h           | -6.057        | -44.231      | 3              | VAL31, SER80, TYR78        | 3.31, 2.39       |
| 2i           | -5.391        | -42.265      | 1              | Tyr78                      | -                |
| Capecitabine | -6.387        | -44.231      | 2              | VAL31, ASP33               | 1.96, 2.01, 3.14 |

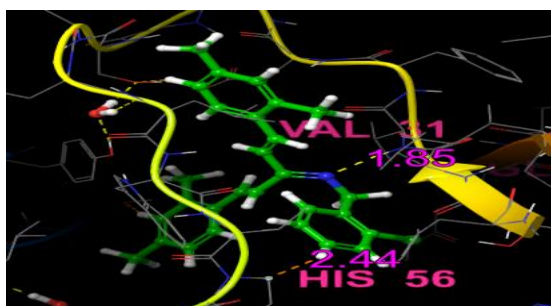


Fig1.3d interaction diagram of 2c with 4OD9

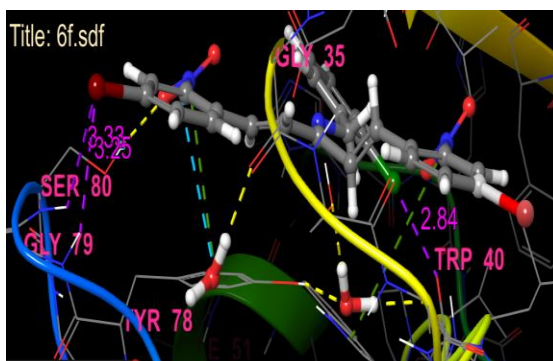


Fig2.3d interaction diagram of 2f with 4OD9

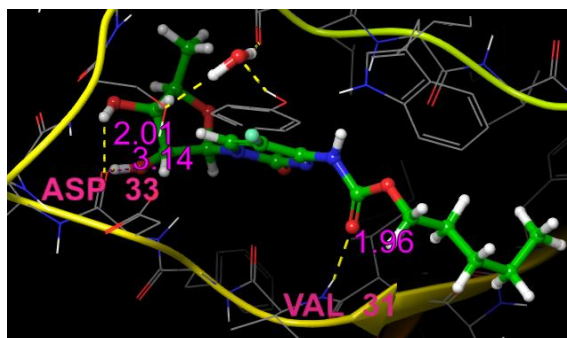


Fig3.3d interaction diagram of Capecitabine with 4OD9

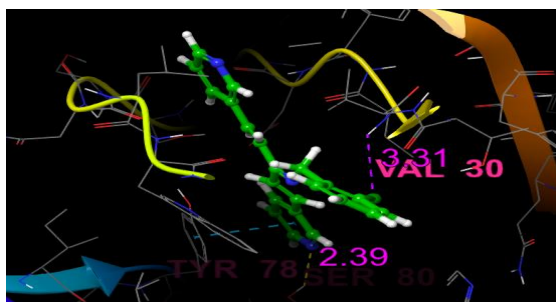
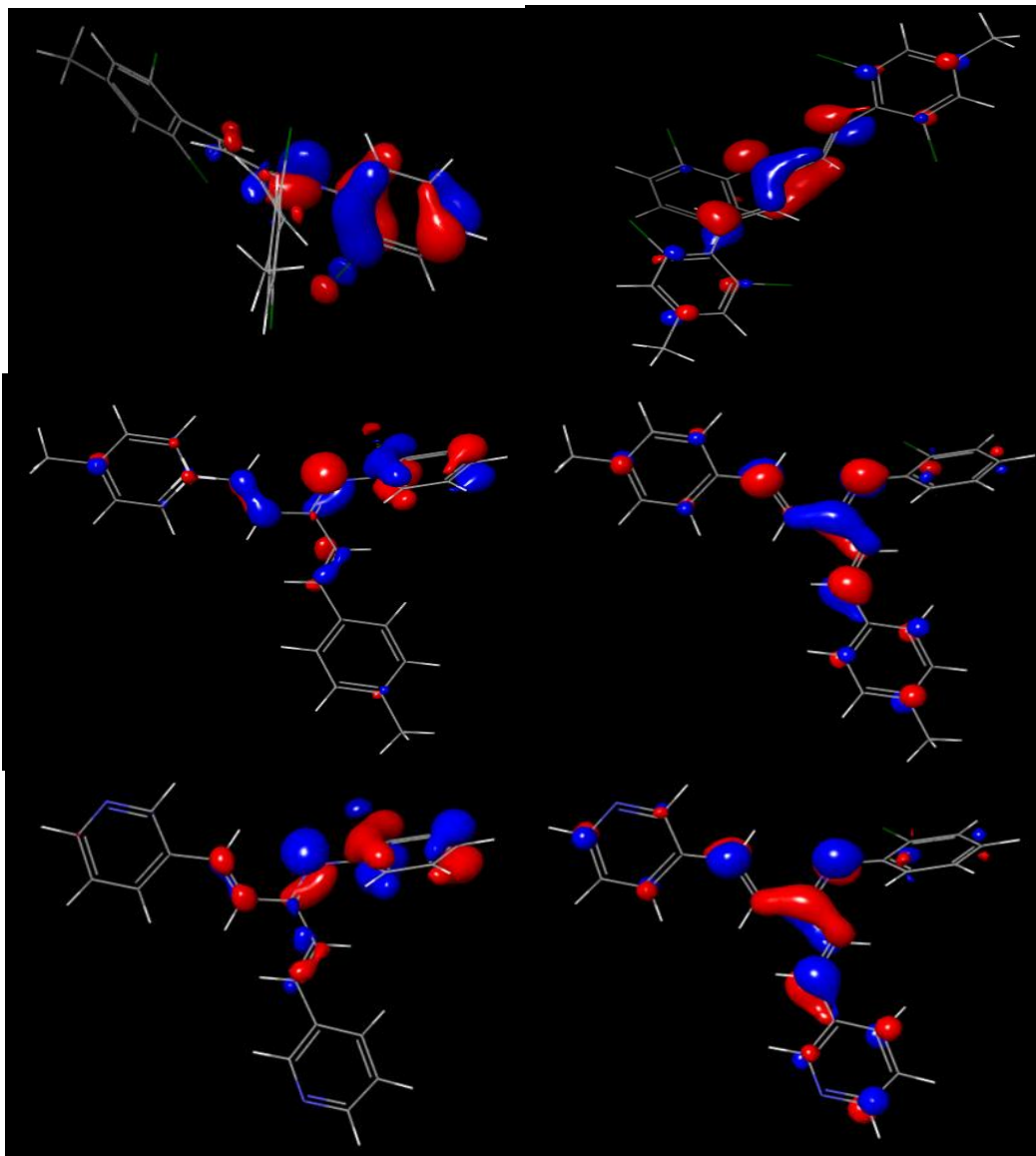


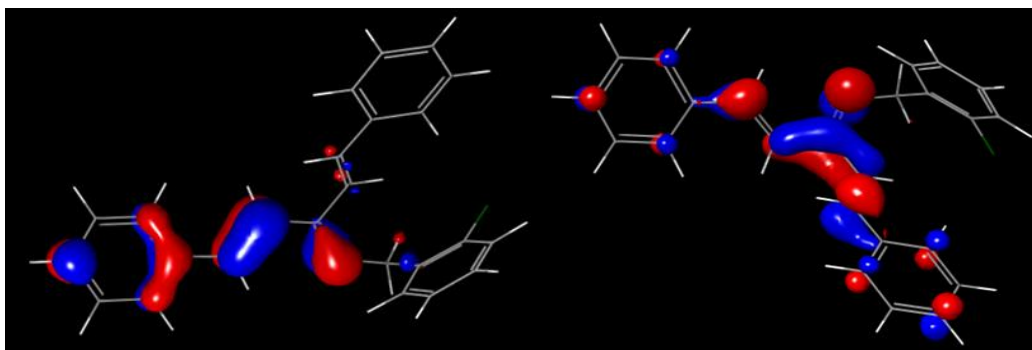
Fig4. 3d interaction diagram of 2h with 4OD9

### HOMO-LUMO

The energy levels of the molecular orbitals order HOMO and LUMO ILs give information on the possible electronic transition. The HOMO and LUMO also indicate the electrophilic and nucleophilic attraction region in molecule shown in Figure 4. The LUMO-HOMO gap is the most important parameter for the chemical reactivity. The shorter LUMO- HOMO gap is considered as the high reactivity.

Figure 4. HOMO, LUMO Diagram of 2e,2f, 2g and 2h





The data of HOMO, LUMO for different energy levels is listed in Table 3

| COMPOUND | HOMO     | LUMO     | $\Delta E$ |
|----------|----------|----------|------------|
| 2e       | -0.20805 | -0.08358 | 0.29163    |
| 2f       | -0.20358 | -0.07551 | 0.27909    |
| 2g       | -0.21759 | -0.09098 | 0.30857    |
| 2h       | -0.21403 | -0.06859 | 0.28262    |

### Chemical reactivity by DFT calculations

The Energy of the HOMO is directly related to the ionization potential and LUMO Energy is directly related to the electron affinity. Energy difference between HOMO and LUMO orbital is called as energy gap which is an important parameter that determines the stability of the structures. The energy gap is used in determining molecular electrical transport properties. In addition, according to Koopmans' theorem the energy gap,  $E_{\text{gap}}$ , defined as the difference between HOMO and LUMO energy [37].

$$E_{\text{gap}} = (E_{\text{LUMO}} - E_{\text{HOMO}}) \approx \text{IP} - \text{EA}$$

The ionization potential (I) and electron affinity (A) can be estimated from the HOMO and LUMO energy values as following equation no 1 and 2. The data of HOMO, LUMO gap, ionization potential, and electron affinity are given in Table 4.

$$I = -E_{\text{HOMO}} \quad \text{..... (1)}$$

$$A = E_{\text{LUMO}} \quad \text{.....(2)}$$

Table4

|    | Ionization Potential (I), eV | Electron Affinity(A), eV |
|----|------------------------------|--------------------------|
| 2e | 0.20805                      | 0.08358                  |
| 2f | 0.20358                      | 0.07551                  |
| 2g | 0.21759                      | 0.09098                  |
| 2h | 0.21403                      | 0.06859                  |

The HOMO and LUMO energies are used for the determination of global reactivity descriptors. It is important that electro-philicity ( $\omega$ ), chemical potential ( $\mu$ ), electro-negativity ( $\chi$ ), hardness ( $\eta$ ) and softness ( $S$ ) be put into a molecular

orbital's framework [38]. We focus on the HOMO and LUMO energies in order to determine the interesting molecular/atomic properties and chemical quantities. These are calculated as following equations given in Table 5.

$$(\mu) = -I + A/2 \quad \dots (3)$$

$$(\eta) = I - A/2 \quad \dots (4)$$

$$(S) = 1/\eta \quad \dots (5)$$

$$(x) = I + A/2 \quad \dots (6)$$

$$(\omega) = \mu^2/2\eta \quad \dots (7)$$

Table 5. Biological and chemical reactivity

|    | Hardness<br>( $\eta$ ) | Softness<br>( $S$ ) | Electrophilicity<br>( $\omega$ ) | Chemical<br>Potential<br>( $\mu$ ) | Electronegativity<br>( $x$ ) |
|----|------------------------|---------------------|----------------------------------|------------------------------------|------------------------------|
| 2e | 0.062235               | 16.06812            | 0.170820                         | -0.145815                          | 0.145815                     |
| 2f | 0.064035               | 15.61645            | 0.152048                         | -0.139545                          | 0.139545                     |
| 2g | 0.063305               | 15.79654            | 0.188009                         | -0.154285                          | 0.154285                     |
| 2h | 0.07272                | 13.75137            | 0.137297                         | -0.14131                           | 0.14131                      |

### Thermo physical properties

The binding free energy of the optimized molecules is calculated by performing docking process. The molecule with minimum binding energy will have the maximum binding affinity. The binding free energy of the designed molecules is obtained by eliminating the energy of the main molecule. Having the maximum binding affinity, indicating as the best molecule for drug leads molecules targeting computationally. We can find out the drug binding affinity by using the fitness of the drug, which can bind to the target molecule during the docking process and the second way is using Gibbs free energy calculations. According to this more negative value, we can consider a more effective drug. The thermo-physical properties like total energy, entropy, free energy, enthalpy, are provided Table 6.

Table 6. Thermophysical Properties

|    | Total energy,<br>(kcal/mol) | Entropy,<br>(kcal/mol-deg)<br>298.15k 1.0atm | Free energy,<br>(kcal/mol)<br>(kcal/mol)<br>298.15k 1.0atm | Enthalpy<br>(kcal/mol)<br>298.15k 1.0atm |
|----|-----------------------------|--|--|--|
| 2e | -3318.98                    | 182.538                                      | -35.8691   | 18.55463                                 |
| 2f | -1480.92                    | 161.876                                      | -32.7267   | 15.53652                                 |
| 2g | -1434.07                    | 146.248                                      | -30.3594   | 13.24436                                 |
| 2h | -1441.19                    | 150.703                                      | -30.8848   | 14.04735                                 |

### Conclusion

The synthesized compounds were characterized by  $^1\text{H}$  NMR,  $^{13}\text{C}$  NMR, IR and Mass spectral analysis. The results obtained from this study confirmed the product Schiff bases were formed. Henceforth viewing these characteristic properties, all

the compounds have variety of biological activity viz., antimicrobial, antifungal, antiinflammatory and anticancer, etc. To sum up, it is concluded that the biological chemistry, chemical reactivity and molecular orbital study like QSAR, HOMO, LUMO, HOMO-LUMO gap, ionization potential, electron affinity, and electrostatic potential in case of the charge distribution in molecule were optimized. From the data it is found that all pyrazole derivatives show highly bioactivity. From docking studies compound 2f shows highly active for breast cancer.

## References

1. Alam R, Wahi D, Singh R, Sinha D, Tandon V, Grover A, Rahisuddin(2016) Bioorg Chem 69:77–90
2. Baviskar AT, Banerjee UC, Gupta M, Singh R, Kumar S, GuptaMK, Kumar S, Raut SK, Khullar M, Singh S, Kumar R (2013) Bioorg Med Chem 21:5782–5793
3. Baviskar AT, Madaan C, Preet R, Mohapatra P, Jain V, Agarwal A(2011) J Med Chem 54:5013–5030
4. Bronson J, Dhar M, Ewing W, Lonberg N (2012) Annu Rep MedChem 47:499–569
5. Friesner RA, Banks JL, Murphy RB, Halgren TA, Klicic JJ, MainzDT, Repasky MP, Knoll EH, Shelley M, Perry JK, Shaw DE, FrancisP, Shenkin PS (2004) J Med Chem 47:1739–1749
6. Glide, version 5.5, Schrödinger, LLC, New York, NY, 2009.
7. How FN, Ibrahim Z and Zulkifli N (2019). Molecular docking of substituted Schiff bases derived from S-benzylidithiocarbazate as potential anticancer agents. *Front. Pharmacol. Conference Abstract: International Conference on Drug Discovery and Translational Medicine 2018 (ICDDTM '18) "Seizing Opportunities and Addressing Challenges of Precision Medicine"*. doi: 10.3389/conf.fphar.2018.63.00100
8. Impact, version 5.5, Schrödinger, LLC, New York, NY, 2005.
9. Jain AN (2006) Curr Protein Pept Sci 7:407–420
10. Kucukguzel SG, Senkardes S (2015) Eur J Med Chem 97:786–815
11. Legentil L, Benel L, Bertrand V, Lesur B, Delfourne E (2006) J MedChem 49:2979–2988
12. LigPrep, version 2.3, Schrödinger, LLC, New York, NY, 2009
13. McNutt MC, Kwon HJ, Chen C, Chen JR, Horton JD, Lagace TA(2009) J Biol Chem 284:10561–10570
14. Momenimovahed Z, Ghoncheh M, Pakzad R, Hasanpour H, Salehiniya H. Incidence and mortality of uterine cancer and relationship with human development index in the world. *Cukurova Med J.* 2017;42(2):233–240. doi:10.17826/cutf.322865
15. Raffa D, Maggio B, Raimondi MV, Cascioferro S, Plescia F, Cancemi G, Daidone G (2015) Eur J Med Chem 97:732–746
16. Ratnawati, I. G. A. A., Sutapa, G. N., & Ratini, N. N. (2018). The concentration of radon gas in air-conditioned indoor: Air quality can increase the potential of lung cancer. *International Journal of Physical Sciences and Engineering*, 2(2), 111–119. <https://doi.org/10.29332/ijpse.v2n2.169>
17. Sachin S. Wazalwar<sup>1</sup> · Anita R. Banpurkar<sup>1</sup> · Franc Perdih, Synthesis, Characterization, Molecular Docking Studies and Anticancer Activity of Schiff

- Bases Derived from 3-(Substituted phenyl)-1-phenyl-1*H*-pyrazole-4-carbaldehyde and 2-Aminophenol, *Journal of Chemical Crystallography*, 13 August 2018
18. Schrödinger Suite 2009 Protein Preparation Wizard; Epik version 2.0, Schrödinger, LLC, New York, NY, 2009.
  19. Sharma A, Shah MK (2013) Synthesis. *Chem Sci Trans*2(3):871–876.
  20. Suryasa, I. W., Rodríguez-Gámez, M., & Koldoris, T. (2021). Get vaccinated when it is your turn and follow the local guidelines. *International Journal of Health Sciences*, 5(3), x-xv. <https://doi.org/10.53730/ijhs.v5n3.2938>
  21. Thaib, P. K. P., & Rahaju, A. S. (2022). Clinicopathological profile of clear cell renal cell carcinoma. *International Journal of Health & Medical Sciences*, 5(1), 91-100. <https://doi.org/10.21744/ijhms.v5n1.1846>
  22. Vichai V, Kirtikara K (2006) *Nat Protoc* 1:1112–1116
  23. Zhang WM, Xing M, Zhao TT, Ren YJ, Yang XH, Yang YS, Lv PC, Zhu HL (2014) *RSC Adv* 4:37197–37207